Journal of Japan Association for Earthquake Engineering, Vol. 24, No. 7, 2024

NONLINEAR SOIL BEHAVIOR AT KIK-NET TOGI OBSERVATION SITE DURING THE 2024 NOTO HANTO EARTHQUAKE

Hidenori MOGI[1]

[1] Member, Dr. Eng., Associate Professor, Graduate School of Science and Engineering, Saitama University, Saitama, Japan, hmogi@jgsk-kmt.sakura.ne.jp

ABSTRACT: We applied NIOM analysis to the earthquake records at the KiK-net Togi site to examine nonlinear behavior of the ground during the 2024 Noto Hanto earthquake. Results revealed that (1) S-wave propagation times increased from 0.2365 s (NS) and 0.2333 s (EW) before the mainshock to 0.3136 s and 0.3245 s, respectively, during principal motion, and (2) S-wave propagation times at the end of the waveform were larger than those before the mainshock by 6 to 6.5%. In addition, a SHAKE91 analysis indicated that (3) the effect of nonlinear behavior was remarkable in the soil layer from GL −28 to −50 m.

Keywords: *The 2024 Noto Hanto earthquake, KiK-net Togi observation site, Nonlinear soil behavior, NIOM method*

1. INTRODUCTION

The M_j 7.6 Noto Hanto (Noto Peninsula) earthquake of January 1, 2024 caused widespread damage centered about the Noto region. The National Research Institute for Earth Science and Disaster Resilience (NIED) maintains KiK-net (Kiban-Kyoshin Net) observation sites[1)] in the epicentral region, and mainshock records were obtained at multiple sites. A KiK-net site consists of vertical-array observation equipment having accelerometers at the surface and in a borehole. The earthquake recordings obtained in this way are extremely valuable for studying the propagation characteristics of seismic waves in a large strain level. From among these KiK-net sites, this report examined the recordings obtained at the KiK-net Togi (ISKH04) site and investigated the nonlinear behavior of the ground accompanying strong motion using the Normalized Input-Output Minimization (NIOM) method developed by Kawakami et al.[2),3)]

2. OBSERVATION SITE AND EARTHQUAKE RECORDS

In this report, from among earthquake records obtained at the KiK-net Togi site from 2017 to January 1, 2024, we analyzed 74 earthquake records each within an epicentral distance R of 200 km. Source parameters[4)] and maximum accelerations of surface seismometer at the KiK-net Togi site are listed in Table 1. The reason why we used records from 2017 on is that there was a period of missing data that lasted for about four years prior to 2017, and we considered the possibility that observations conditions

Table 1 Source parameters of analyzed earthquakes[4] and maximum accelerations of surface seismometer

No.	Date/Time (JST) (Y/M/D H:M:S)	D (km)	M	R (km)	Max. Acc. (cm/s²) NS	EW	UD	Geographical region
1	2017/04/01 19:43:23	5.1	3.6	14.4	5.86	6.12	2.80	NOTO PENINSULA REG
2	2017/06/25 07:02:15	6.7	5.6	166.1	3.24	4.21	1.51	WESTERN NAGANO PREF
3	2017/09/08 12:42:16	7.1	3.6	11.6	7.63	6.39	3.37	NOTO PENINSULA REG
4	2017/11/09 12:23:54	15.7	3.7	19.0	10.32	3.85	2.72	NOTO PENINSULA REG
5	2018/01/05 11:02:23	13.7	4.0	42.4	5.15	1.45	1.75	TOYAMA PREF
6	2020/03/13 02:18:47	12.3	5.5	13.7	130.34	130.58	43.41	NOTO PENINSULA REG
7	2020/03/13 04:53:07	12.1	3.5	13.9	4.13	2.85	1.89	NOTO PENINSULA REG
8	2020/04/06 05:00:09	12.1	4.0	12.0	28.35	17.96	10.40	NOTO PENINSULA REG
9	2020/05/19 13:12:58	2.5	5.4	129.3	1.12	1.42	0.36	HIDA MOUNTAINS REG
10	2020/05/19 16:55:08	1.8	4.7	126.5	0.98	0.58	0.27	HIDA MOUNTAINS REG
11	2020/05/29 19:05:15	3.7	5.3	131.8	0.75	0.80	0.21	HIDA MOUNTAINS REG
12	2020/09/02 02:49:58	8.5	4.6	82.4	1.73	1.91	1.10	ISHIKAWA PREF
13	2020/09/04 09:10:53	7.1	5.0	128.3	2.69	2.90	0.62	CENTRAL FUKUI PREF
14	2021/06/03 10:31:52	15.3	4.1	39.9	2.70	2.24	1.47	TOYAMA BAY REG
15	2021/06/26 01:24:55	13.5	4.1	58.0	1.95	1.02	0.84	NOTO PENINSULA REG
16	2021/07/11 09:16:41	12.9	3.9	60.1	3.64	1.87	2.53	NOTO PENINSULA REG
17	2021/08/14 22:38:07	13.5	4.2	57.1	1.28	0.86	0.60	NOTO PENINSULA REG
18	2021/09/07 14:07:07	13.3	4.2	57.6	2.72	1.99	0.50	NOTO PENINSULA REG
19	2021/09/16 18:42:30	13.1	5.1	62.4	14.68	10.55	4.39	NOTO PENINSULA REG
20	2021/09/19 17:18:30	0.0	5.3	123.9	0.95	0.72	0.36	HIDA MOUNTAINS REG
21	2021/10/03 11:10:59	13.2	4.3	57.7	2.25	1.53	0.99	NOTO PENINSULA REG
22	2021/10/19 15:03:07	13.2	4.0	56.9	0.90	0.59	0.66	NOTO PENINSULA REG
23	2021/10/22 21:51:33	14.8	3.5	58.2	0.71	1.42	0.45	ISHIKAWA PREF
24	2021/11/05 00:21:49	13.0	4.0	57.7	1.07	0.99	0.47	NOTO PENINSULA REG
25	2021/12/31 14:52:43	13.8	4.3	58.8	1.16	0.76	0.37	NOTO PENINSULA REG
26	2022/02/07 17:59:24	13.5	4.1	58.7	1.10	0.59	0.85	NOTO PENINSULA REG
27	2022/03/07 16:36:07	10.3	3.4	56.4	0.92	1.02	0.44	NOTO PENINSULA REG
28	2022/03/08 01:06:27	10.6	3.9	56.4	5.05	3.57	2.10	NOTO PENINSULA REG
29	2022/03/08 01:58:50	13.5	4.8	59.1	4.44	2.87	1.55	NOTO PENINSULA REG
30	2022/03/10 19:32:08	12.8	3.7	62.2	1.26	0.52	0.38	NOTO PENINSULA REG
31	2022/03/23 09:23:57	13.8	4.3	62.9	1.64	0.91	0.75	NOTO PENINSULA REG
32	2022/04/04 10:26:25	13.9	4.3	57.8	1.29	0.73	0.41	NOTO PENINSULA REG
33	2022/04/04 10:28:08	13.1	4.0	57.2	1.66	0.63	0.36	NOTO PENINSULA REG
34	2022/04/08 22:04:58	13.3	4.2	61.5	2.96	2.31	1.03	NOTO PENINSULA REG
35	2022/05/20 19:58:18	13.6	4.1	64.4	1.54	1.02	0.43	NOTO PENINSULA REG
36	2022/06/19 15:08:08	13.1	5.4	61.2	13.11	10.08	5.11	NOTO PENINSULA REG
37	2022/06/20 10:31:34	13.9	5.0	65.0	11.51	9.53	4.59	NOTO PENINSULA REG
38	2022/06/20 14:50:14	13.8	4.3	64.7	3.62	2.71	1.64	NOTO PENINSULA REG
39	2022/06/21 10:42:51	12.4	4.1	60.3	3.64	4.07	1.37	NOTO PENINSULA REG
40	2022/08/14 19:14:02	13.1	4.1	58.1	0.43	0.61	0.27	NOTO PENINSULA REG
41	2022/08/14 19:28:29	13.1	3.9	58.4	1.60	0.92	0.46	NOTO PENINSULA REG
42	2022/11/14 22:27:59	11.9	4.2	60.4	1.13	1.23	0.74	NOTO PENINSULA REG
43	2022/11/24 05:13:55	13.2	3.9	56.9	1.04	0.63	0.59	NOTO PENINSULA REG
44	2022/11/26 21:58:13	12.8	4.2	59.3	1.36	1.21	0.34	NOTO PENINSULA REG
45	2022/11/30 17:07:02	13.7	4.4	47.8	4.00	2.29	1.29	NOTO PENINSULA REG
46	2022/12/09 05:58:07	12.1	4.1	62.7	1.01	1.04	0.39	NOTO PENINSULA REG
47	2022/12/18 00:53:58	12.6	3.9	47.4	1.09	0.77	0.46	NOTO PENINSULA REG
48	2023/01/06 13:44:04	13.4	4.5	60.6	8.61	7.25	2.50	NOTO PENINSULA REG
49	2023/01/14 10:22:33	13.7	3.5	60.3	0.75	0.41	0.38	NOTO PENINSULA REG
50	2023/02/21 22:53:48	11.5	4.1	61.7	0.92	0.88	0.55	NOTO PENINSULA REG
51	2023/03/29 03:48:16	12.8	4.1	63.7	1.56	1.18	0.54	NOTO PENINSULA REG
52	2023/05/05 14:42:04	12.1	6.5	64.8	37.12	19.93	16.96	NOTO PENINSULA REG
53	2023/05/05 14:47:48	13.1	4.0	64.7	1.28	0.43	0.54	NOTO PENINSULA REG
54	2023/05/05 14:53:37	12.8	5.0	58.2	6.15	3.05	1.77	NOTO PENINSULA REG
55	2023/05/05 15:06:34	13.9	3.9	66.3	1.20	0.71	0.39	NOTO PENINSULA REG
56	2023/05/05 17:38:02	13.5	4.3	68.8	1.80	1.37	0.60	OFF NOTO PENINSULA
57	2023/05/05 21:58:04	13.7	5.9	59.1	26.11	16.69	11.29	NOTO PENINSULA REG
58	2023/05/05 22:03:38	11.7	4.0	59.0	0.99	0.48	0.30	NOTO PENINSULA REG
59	2023/05/05 22:26:47	13.2	4.1	57.3	0.73	0.71	0.48	NOTO PENINSULA REG
60	2023/05/05 22:33:59	13.2	4.0	57.6	1.12	0.83	0.50	NOTO PENINSULA REG
61	2023/05/05 22:33:59	13.2	4.0	57.6	1.12	0.83	0.50	NOTO PENINSULA REG
62	2023/05/05 22:51:43	12.9	3.8	61.1	0.73	0.52	0.27	NOTO PENINSULA REG
63	2023/05/05 23:18:51	13.8	4.3	56.2	2.24	2.89	0.96	NOTO PENINSULA REG
64	2023/05/06 23:54:01	11.5	4.1	66.6	1.04	0.95	0.45	OFF NOTO PENINSULA
65	2023/05/09 05:14:19	14.5	4.7	64.0	4.61	4.85	2.05	NOTO PENINSULA REG
66	2023/05/09 05:16:15	13.9	4.4	64.9	7.97	6.27	1.89	NOTO PENINSULA REG
67	2023/05/09 11:05:55	8.8	4.2	64.9	1.07	0.87	0.49	OFF NOTO PENINSULA
68	2023/05/10 07:14:39	12.3	4.9	67.9	6.94	5.76	3.15	OFF NOTO PENINSULA
69	2023/05/10 21:54:48	12.7	5.0	72.0	2.89	2.12	0.69	OFF NOTO PENINSULA
70	2023/05/22 00:20:27	11.3	4.0	68.6	1.43	0.69	0.28	OFF NOTO PENINSULA
71	2023/05/30 17:49:16	4.5	4.6	69.4	0.76	1.22	0.65	OFF NOTO PENINSULA
72	2023/07/08 21:36:06	13.5	4.0	58.0	1.46	0.52	0.59	NOTO PENINSULA REG
73	2023/09/28 23:29:48	12.3	4.3	55.0	1.28	1.32	0.55	NOTO PENINSULA REG
74	2024/01/01 16:10:23	15.9	7.6	55.0	511.6	483.7	1201.9	NOTO PENINSULA REG

(Continued)

D : Focal depth, *M* : JMA magnitude, *R* : Epicentral distance

had changed since then. The deviation in the installation direction of the borehole seismometer at the KiK-net Togi site was small at −1°, so in this report, no compensation was made for the installation orientation.

Figure 1 shows (a) the epicenter distribution of analyzed earthquakes and waveforms recorded at the KiK-net Togi site for (b) the earthquake of September 28, 2023 (focal depth *D* 12.3 km, *M* 4.3, *R* 55

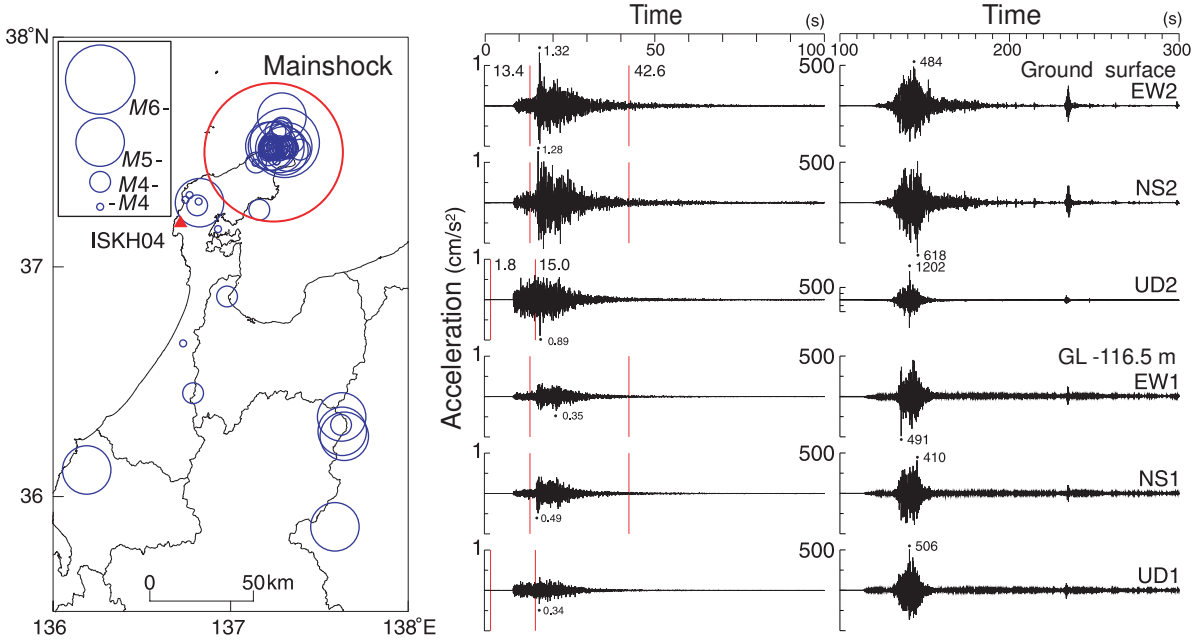

(a) Epicenters and ISKH04 site (b) Sep. 28, 2023 *M* 4.3 (c) Jan. 1, 2024 *M* 7.6

Fig. 1 Epicenters of analyzed earthquakes and examples of observed waveforms at KiK-net Togi site

km) and (c) the 2024 Noto Hanto earthquake (*D* 15.9 km, *R* 55 km). The recordings for (c) the 2024 Noto Hanto earthquake show maximum acceleration underground (GL −116.5 m) reached a value of 400–500 cm/s^2 indicating the occurrence of extremely strong motion. In addition, the recordings for the (b) September 28, 2023 earthquake revealed that the surface waveforms were about three times the maximum acceleration underground for all three components indicating a ground amplification effect. In contrast, the recordings for (c) the 2024 Noto Hanto earthquake showed an amplification of about two times in the vertical component while no major amplification could be seen in the horizontal components, which confirmed the nonlinear behavior of the ground due to strong motion.

3. NIOM ANALYSIS

The NIOM method[2),3)] takes earthquake observation recordings obtained simultaneously from two points to estimate wave propagation times between those points. Details of this analysis parameters are similar to that described in Mogi et al.,[5)] but in this report, the recording of the underground seismograph at time 0 is replaced by a pulse wave (input model) as unit amplitude and the positive peak time of the surface simplified waveform (output model) corresponds to the propagation time of the up-going wave.

Figure 2 shows examples of NIOM analysis results. In the figure, (a) shows results for the minor earthquake of September 28, 2023 (as shown by the red lines in Fig. 1 (b), the analysis time window is set to about 20 s including the S-wave arrival for the horizontal components, but for the vertical component, it is set so as to include the P-wave arrival but not the S-wave arrival). Additionally, for the recordings of the 2024 earthquake, the analysis was performed from 113 s immediately before the P-wave arrival to 293 s while moving a 4-s time window in 2-s increments. Here, (b), (c), and (d) show results for the P-wave portion (113–117 s in Fig. 1 (c)), principal motion portion (141–145 s), and coda portion (271–275 s) , respectively. In the figure, the red, blue, and solid black lines indicate the output model (surface simplified waveform) of the NS, EW, and UD components, respectively, and the broken line indicates the input model (underground simplified waveform) of the NS component. Although NIOM analysis is performed using recordings of components in the same direction by the surface and borehole seismometers, only the results for the NS component are shown here for the input model. As revealed by these results, clear peaks can be seen in the output model for all three components. In the (c) principal motion portion of the 2024 earthquake, propagation times are long and peak amplitudes are small, but this is due to a decrease in shear rigidity and increase in attenuation owing to strong motion.

Figure 3 (a) shows the results of analyzing the records of 73 earthquakes from 2017 to 2023. It can be seen from these results that stable propagation times were obtained. The results for earthquake numbers 6, 7, and 52 show long propagation times, these are due to nonlinearity and its residual effect during the 2:18 *M* 5.5 and 4:53 *M* 3.5 on March 13, 2020, and 14:42, May 5, 2023 *M* 6.5 earthquakes of the Noto earthquake swarm. The average values of the obtained propagation times are 0.2365 s, 0.2333 s, and 0.0529 s for NS, EW and UD components, respectively.

Figure 3 (b) shows the temporal change of propagation times during the 2024 Noto Hanto earthquake.

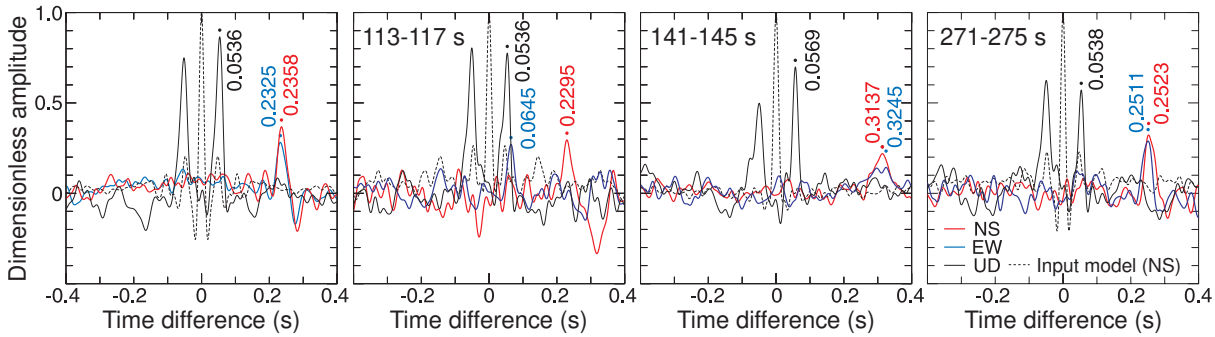

(a) Sep. 28, 2023 23:29 *M*4.3 (b) Mainshock, P-wave portion (c) Principal motion portion (d) Coda portion

Fig. 2 Examples of NIOM analysis results

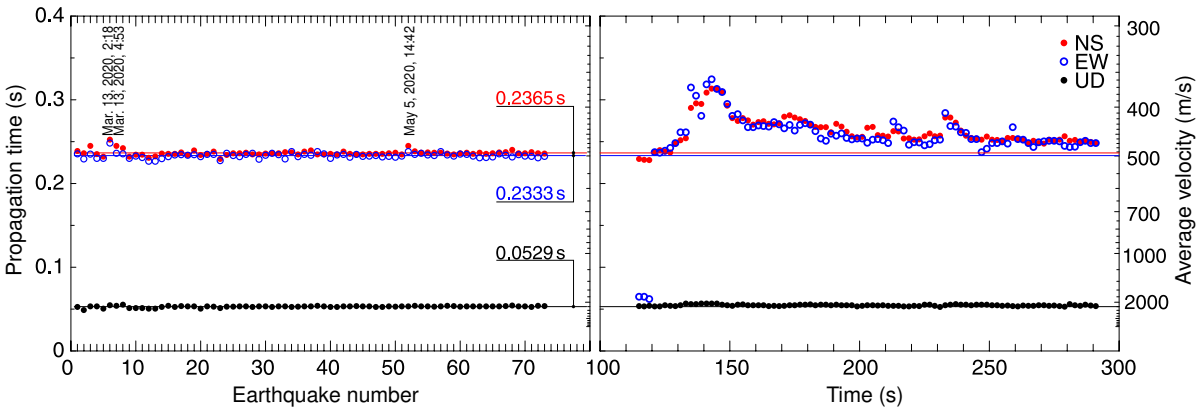

(a) Earthquakes from 2017 to 2023 (b) The 2024 Noto Hanto Earthquake

Fig. 3 Propagation times obtained by NIOM analysis (the horizontal lines in the figure indicate average propagation times for earthquakes prior to the 2024 Noto Hanto earthquake)

The values obtained were nearly the same as the average values shown in Fig. 3 (a) up to the 15 s after the P-wave arrival. For the horizontal components, propagation times increased greatly at 135 s of the waveform, and after reaching maximum values (NS component: 0.3136 s; EW component: 0.3245 s) at 143 s, they decreased together with a drop in the amplitude of earthquake motion. However, at the end of the waveform, these propagation times did not return to their values before the mainshock (NS component: 0.2511 s; EW component: 0.2484 s), so it could be seen that the effects of ground nonlinearity remained. This residual amount was 6 to 6.5% of the propagation times before the mainshock. For the UD component, however, propagation times were nearly constant despite the strong motion, so it could be seen that P-wave velocity was hardly affected even for such remarkable acceleration at this site. Furthermore, a sudden increase in propagation times can be seen at 233 s of the waveform for the horizontal components, this is attributed to a strong aftershock included in the mainshock recordings.

4. EQUIVALENT LINEAR ANALYSIS BY SHAKE91

To investigate which layer brought about an increase in the propagation times obtained by NIOM analysis, we performed equivalent linear analysis using the SHAKE91 program. Our initial model was based on the results of KiK-net PS logging (five-layer model), but on using this S-wave velocity, the propagation time between seismographs turned out to be 0.1936 s, which was smaller than that during normal times by NIOM analysis. For this reason, we adjusted this PS-logging S-wave velocity by uniformly multiplying it by a coefficient (the ratio of 0.1936 s over 0.2349 s (0.1936/0.2349), where the denominator is the average value of the NS and EW components before the mainshock by NIOM analysis

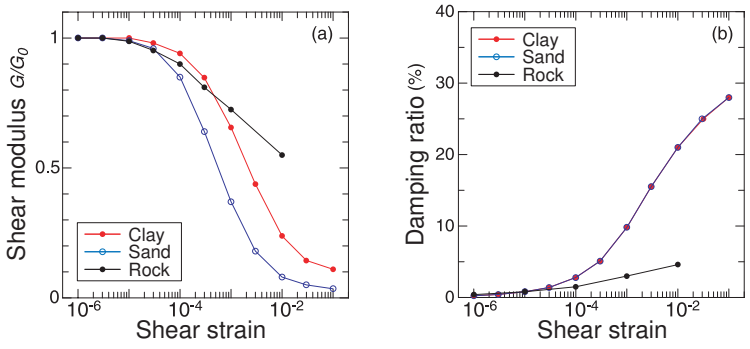

Fig. 4 Strain dependence of shear modulus and damping ratio used in this report[6)]

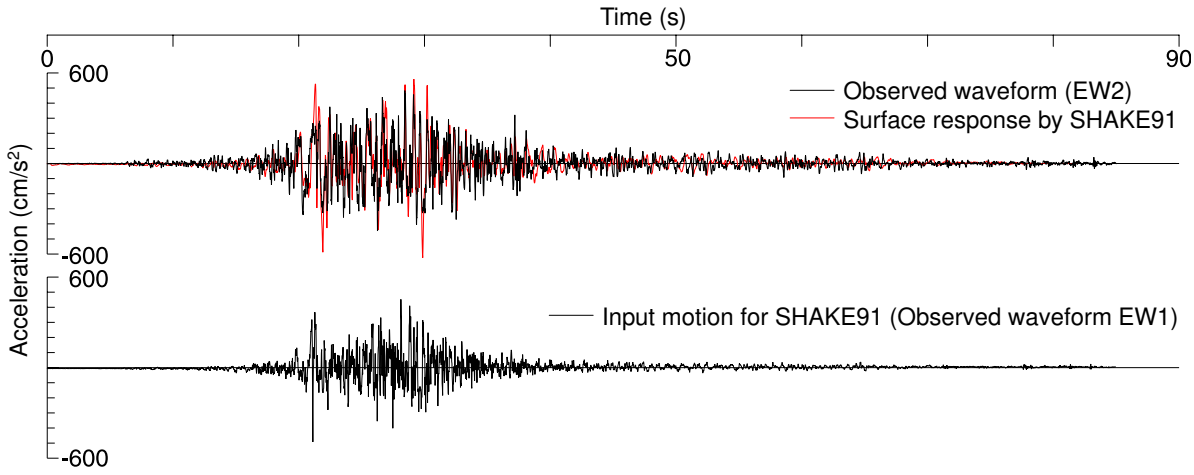

Fig. 5 Comparison of surface response waveform by SHAKE91 and observed waveform

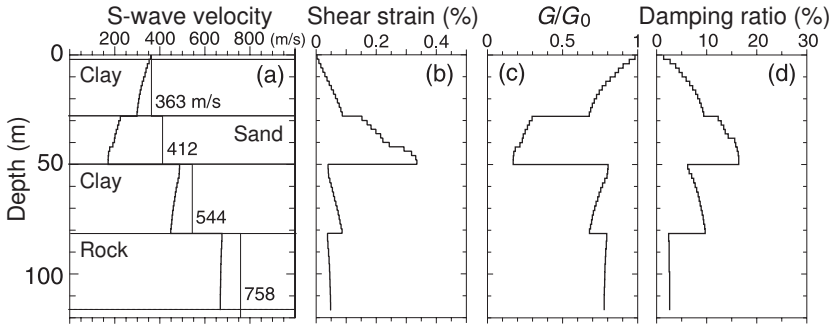

Fig. 6 Depth distribution of physical properties by SHAKE91

shown by the horizontal lines in Fig. 3 (Fig. 6 (a) shows this velocity). This five-layer model consists, in order from the surface, two clay layers, a sand layer, another clay layer, and a soft rock layer. Since the strain dependence of the physical properties of each layer is unknown, we used strain-compatible shear modulus G/G_0 and damping ratio h for each of the above soil qualities taken from examples in SHAKE91 shown in Fig. 4. The effective strain used here for fitting the physical properties was 0.6 times the maximum strain. The input motion was taken to be the 76-s segment following 115 s of the EW component of the borehole observed waveform (EW1) (3,800 data items culled in time steps of 0.02 s), and analysis was performed setting the number of Fourier transform data values to 4,096. The waveform set as input motion, the surface response waveform by SHAKE91, and the surface observed waveform (EW2) are shown in Fig. 5. On comparing the surface response waveform by SHAKE91 and the surface observed waveform (EW2), the two waveforms show good phase correspondence in the principal motion portion, which indicates that change in propagation velocity due to nonlinearity could be simulated. On the other hand, amplitude in the surface response waveform by SHAKE91 is somewhat larger than that in the observed wave, so the possibility exists that the actual damping ratio in the ground is larger than the evaluation value. Both the P-wave portion and coda portion show poor phase correspondence, which verifies that propagation velocity differs from that in the principal motion portion.

The physical properties of each layer obtained by this analysis are shown in Fig. 6. In the figure, (a) shows the initial values (thin solid lines) and convergence values (bold lines) of the S-wave velocity estimated by the SHAKE91 analysis described above, and (b)–(d) show the convergence values of shear strain, the strain-compatible shear modulus (G/G_0), and damping ratio, respectively. The effect of nonlinearity is especially noticeable in the GL −28 to −50 m layer. In the lower part of this layer, G/G_0 decreases to 0.17 and the damping ratio increases to 16% due to a shear strain of about 0.3%. As a result, the magnitude relationship of the S-wave velocity with the upper clay layer switches. Based on this result, propagation time between seismometers is 0.3205 s, which is close to the value obtained

by NIOM analysis. These physical properties were, however, based on the assumed strain dependence shown in Fig. 4. In particular, the large change in rigidity in the sand layer at GL −28 to −50 m could be caused by setting a large modulus reduction rate of the sand layer, so it must be kept in mind that results change according to strain-dependence settings.

5. CONCLUDING REMARKS

We applied NIOM analysis to earthquake records observed at the KiK-net Togi site and investigated nonlinear behavior of the ground during the 2024 Noto Hanto earthquake. Analysis results revealed that (1) S-wave propagation times before the mainshock (NS component: 0.2365 s; EW component: 0.2333 s) increased to 0.3136 s and 0.3245 s, respectively, during mainshock principal motion and (2) propagation times at the end of the waveform were larger than those before the mainshock by 6 to 6.5%. Analysis by the SHAKE91 program indicated that (3) the effect of nonlinear behavior was remarkable in the GL −28 to −50 m layer and (4) propagation times after nonlinearization were consistent with the results of NIOM analysis. It must be kept in mind, however, that SHAKE91 results are based on assumed strain dependence, which means that these results change according to strain-dependence settings.

ACKNOWLEDGMENTS

This report made use of recordings from the KiK-net Togi site operated by the National Research Institute for Earth Science and Disaster Resilience (NIED), the NIOM analysis program developed by Kawakami laboratory of Saitama University, and the SHAKE91 program from the University of California, Berkeley. We extend our deep appreciation to all concerned for the use of these materials.

REFERENCES

1) National Research Institute for Earth Science and Disaster Resilience: *NIED K-NET, KiK-net*, National Research Institute for Earth Science and Disaster Resilience. https://doi.org/10.17598/NIED.0004
2) Kawakami, H. and Haddadi, H. R.: Modeling Wave Propagation by Using Normalized Input-Output Minimization (NIOM), *Soil Dynamics and Earthquake Engineering*, Vol. 17, No. 2, pp. 117–126, 1998.
3) Haddadi, H. R. and Kawakami, H.: Modeling Wave Propagation by Using Normalized Input-Output Minimization (NIOM) Method for Multiple Linear Systems, *Structural Engineering/Earthquake Engineering*, Japan Society of Civil Engineers, Vol. 15, No. 1, pp. 29s–39s, 1998.
4) National Research Institute for Earth Science and Disaster Resilience: *Preliminary Catalog by the Hi-net Automatic System*, National Research Institute for Earth Science and Disaster Resilience. https://hinetwww11.bosai.go.jp/auth/JMA/jmalist.php?LANG=ja (last accessed on January 8, 2024)
5) Mogi, H., Shrestha, S. M., Kawakami, H. and Kawamura, J.: Nonlinear Soil Behavior Examined on the Basis of Propagation Time Observed at the KiK-net Ichinoseki-Nishi Vertical Array, *Bulletin of the Seismological Society of America*, Vol. 103, No.1, pp.180–195, 2013.
6) Idriss, I. M. and Sun, J. I.: User's Manual for SHAKE91—A Computer Program for Conducting Equivalent Linear Seismic Response Analyses of Horizontally Layered Soil Deposits, *NISEE e-Library*, 1992. https://nisee.berkeley.edu/elibrary/getpkg?id=SHAKE91 (last accessed on January 8, 2024)

(Original Japanese Paper Published: August, 2024)
(English Version Submitted: November 01, 2024)
(English Version Accepted: December 08, 2024)